ICIC Express Letters
Part B: Applications
Volume **9**, Number **1**, January **2018**

ICIC International ©2018 ISSN 2185-2766
pp. 1–9

STRUCTURE MODELING AND STATIC ANALYSIS OF A NOVEL LEG-WHEELED RESCUE ROBOT

Hongbo Wang[1,2,*], Jianye Niu[1,2], Yuxiang Zhang[1,2], Dong Li[1,2]
Shanshan Li[1,2] and Shaozhen Wu[1,2]

[1]Parallel Robot and Mechatronic System Laboratory of Hebei Province
[2]Key Laboratory of Advanced Forging & Stamping Technology and Science of Ministry of Education
Yanshan University
No. 438, West Hebei Ave., Qinhuangdao 066004, P. R. China
*Corresponding author: hongbo_w@ysu.edu.cn

Received July 2017; accepted September 2017

Abstract. *This paper presents a novel rescue robot with three degrees of freedom (3-DOF) parallel leg mechanism based on the serial-parallel and leg-wheeled mechanism. It is a two Universal-Prismatic-Spherical plus one Universal and Revolute ((2-UPS+U)&R) serial-parallel mechanism. Firstly, the whole structure and the frame of the robot were described. The key problem of each leg's structure was formulated and solved. Secondly, static analysis of the single leg mechanism was carried out, which includes the calculation of inertial force and torque, and the active force and the reaction force of the upper leg mechanism. Lastly, a numerical example was provided at the end of the paper to show the effectiveness of the proposed method.*
Keywords: Rescue robot, (2-UPS+U)&R, Leg-wheeled mechanism, Structure modeling, Static analysis

1. **Introduction.** In recent years, many disasters such as earthquake, flood, fire, nuclear leak and terrorist activity occurred frequently, which pose a threat to human security and have aroused wide public concern. When the rescue robot appears, it reduces the loss of disasters, and provides the security of the future life. Therefore, many countries in the world research on rescue robots, which has become one of the hot topics in robot field. In Japan, many rescue robots were developed, such as Snakebot [1-3], Quince [4,5] and Roller-Walker [6,7]. In U.S.A, PackBot [8] and Talon [9] were developed. However, the developed rescue robots have very limited flexibility and motion ability, and they cannot do the search and rescue work very well. So the leg-wheeled robot has been widely studied due to its outstanding obstacle crossing ability and great adaptability [10-14]. After summing up the researches of rescue robot, this paper presents a novel leg-wheeled rescue robot, with a (2-UPS+U)&R series-parallel mechanism. The mechanism has the combining advantages of series mechanism (big work space and flexible end-effector) and parallel mechanism (high precision and strong bearing capacity). So it overcomes small work space and can achieve high precision and strong bearing capacity. The serial mechanism and parallel mechanism are combined, it will further expand the application field of robot and it has an important scientific significance and application value. Static analysis is a necessary step for mechanism design, an important means to check whether the new structure model is reasonable, and provides the theoretical basis for the structural parameters optimization [15,16]. In this paper, the static equilibrium equations of the single leg mechanism are established by using vector method. Based on the static analysis of the series-parallel mechanism, the relationships between the driving forces, the external forces and the constraint reaction forces of the pairs were obtained.

2. Structure Modeling of the Leg-Wheeled Rescue Robot.

2.1. Structure model of the robot. Based on the principle of bionics and according to the local and international research on the leg-wheeled hybrid robot, this paper presents an innovative (2-UPS+U)&R serial-parallel and leg-wheeled mechanism, which is used as the robot's leg. Compared to the traditional leg mechanism, the new mechanism adopted the advantages and abandoned the drawbacks of those existing mechanisms. The body structure enables the robot to buffer the impact of the ground in the process of rapid movement. The wheels were installed on the knee joint of the leg mechanism to reduce its influence on the flexibility of the robot. The installation position of wheels can ensure that the flexibility of the lower leg will not be affected, and can take full advantage of the ability to overstep obstacles of the leg mechanism. The transmission systems of the lower leg and the wheel were independent, and different gear ratios were adopted to meet their respective transmission requirements. When the robot moves in the leg mode, the lower legs contact with the ground which is equivalent to a quadruped walking robot. When the robot moves in the wheel mode, the lower leg retracts and the wheels contact with ground, which is equivalent to a four-wheel mobile robot. Its flexibility and carrying capacity are greatly improved, and the 3D model of the leg-wheeled rescue robot is shown in Figure 1(a) and Figure 1(b).

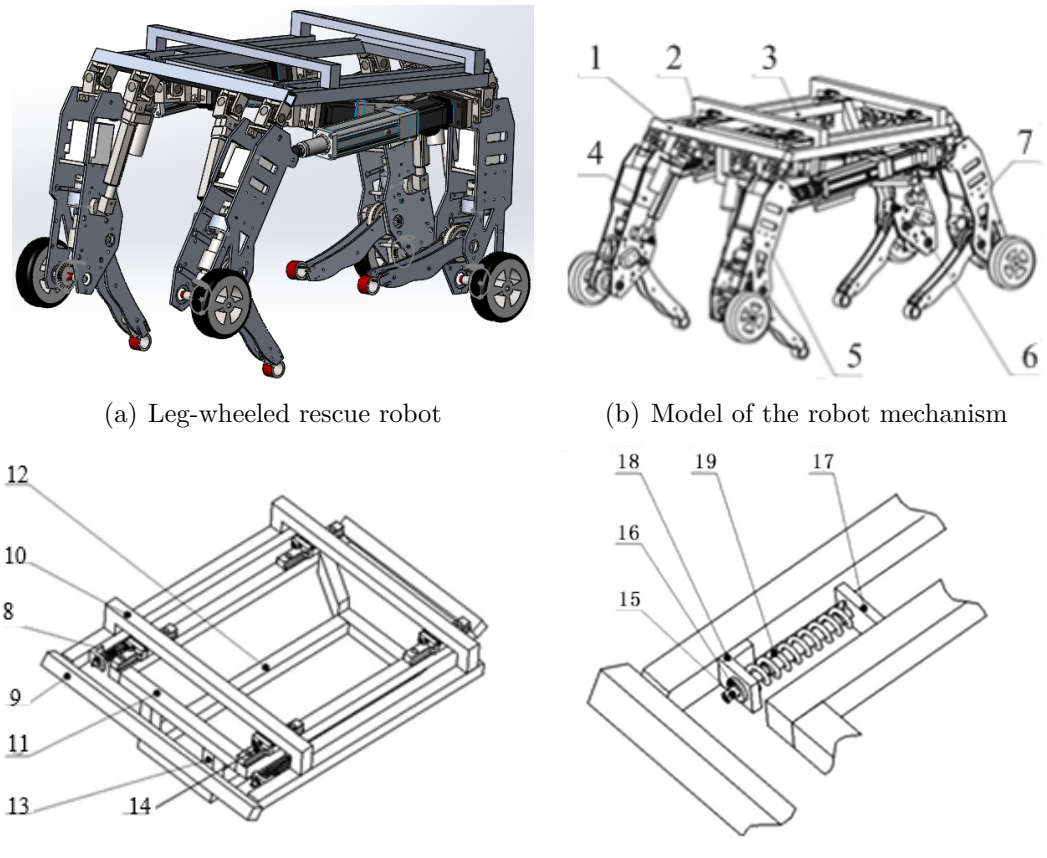

(a) Leg-wheeled rescue robot

(b) Model of the robot mechanism

(c) Structure of the frame

(d) Structure of the buffer components

1-the front frame, 2-the buffer component, 3-the inner frame, 4-the right foreleg, 5-the left foreleg, 6-the right rear leg, 7-the left rear leg, 8-the buffer components, 9-the portal frame, 10-longitudinal rod, 11-the upper rectangle frame, 12-the under rectangle frame, 13-the straight connecting rod, 14-standard linear slider components, 15-buffer screw, 16-the buffer pad, 17-the inner frame link stopper, 18-the front frame link stopper, 19-the buffer spring

FIGURE 1. Structure model of the leg-wheeled rescue robot

The overall frame of the robot is shown in Figure 1(c). The outer frame and the inner frame are connected by the buffer component which can absorb the impact force of the ground and the stored energy can be used in the movement later. The buffer component is shown in Figure 1(d).

2.2. **Model of the leg mechanism.** The leg mechanism must meet the requirements of the flexibility of walking performance, carrying capacity, simple structure and easy control. Based on the bionics theory, the leg mechanism was designed as shown in Figure 2. The two straight push rods mimic the muscle distribution of the leg to drive the upper leg and the front frame mimics the animal body. The straight push rods and the front frame constitute a (2-UPS+U)&R serial-parallel mechanism. With the application of the 2-DOF parallel mechanism, the robot has the advantages of greater transport capacity and a better rigidity with a small coupling. Unlike the wheel installed in the end of the lower leg, the wheel which is installed in the knee joint will not affect the flexibility of the leg movement.

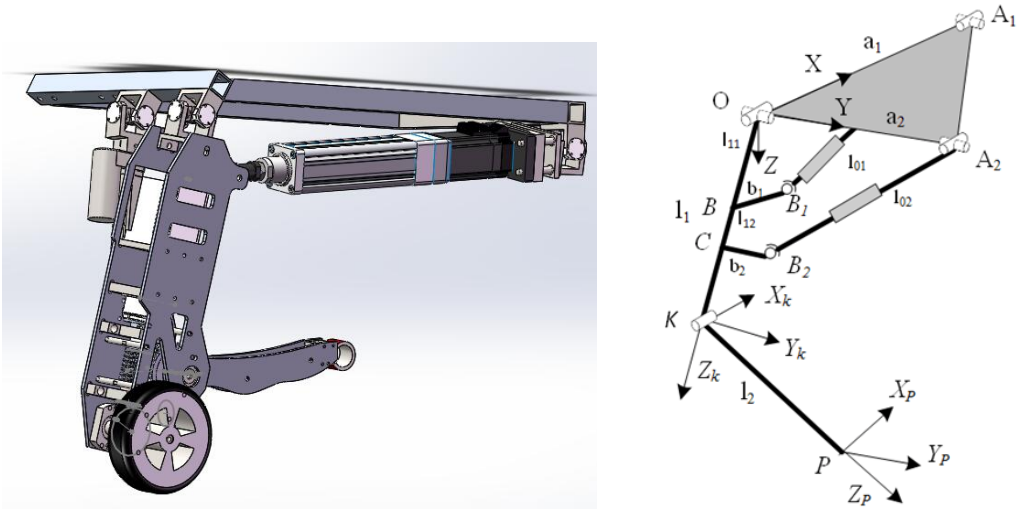

FIGURE 2. Model of the leg mechanism

The upper leg is a 2-DOF (2-UPS+U) parallel mechanism, which consists of a swinging rod with a U-pair (Hooke hinge), a big push rod and a small push rod. Both ends of the big push rod and the small push rod are the U-pair and S-pair (ball hinge) respectively, and the two S-pairs are installed on the upper leg, which form the two UPS mechanism. In the parallel mechanism, the frame is the fixed platform, and the big push rod and the small push rod are branch mechanisms. The upper leg is not only the moving platform, but also the branch mechanism, and possesses a higher carrying capability and a higher structural strength as a novel leg mechanism. The upper leg and lower leg are connected by an R-pair.

3. Static Analysis of the Single Leg Mechanism.

3.1. **Calculation of inertial force and torque.** All the components of the single leg mechanism of the leg-wheeled hybrid rescue robot are always in the process of motion, so the inertia force must be added in order to study the static equilibrium problem in the inertial system. The inertial force and torque at the center of mass of each component of the upper leg mechanism can be expressed as f and T, as follows:

$$f = \begin{bmatrix} f_x & f_y & f_z \end{bmatrix}^{\mathrm{T}}, \quad T = \begin{bmatrix} T_x & T_y & T_z \end{bmatrix}^{\mathrm{T}} \tag{1}$$

f and T can be expressed in the following equations:

$$f_k^i = -m_k a_k, \quad T_k^i = -\left[I_k^o\right]\varepsilon_k - \left[\omega_k\right]\left[I_k^o\right]S\left(\omega_k\right)$$
$$S\left(\omega_k\right) = \begin{bmatrix} 0 & -\omega_z & \omega_y \\ \omega_z & 0 & -\omega_x \\ -\omega_y & \omega_x & 0 \end{bmatrix} \tag{2}$$

where k indicates the number of each bar in the fixed platform and other branches, m indicates the mass of each bar in the fixed platform and other branches, and I_k^o indicates the 3-order inertia matrix of each bar on the origin O of the fixed coordinate system.

All the bars of each branch of the (2-UPS+U)&R series-parallel mechanism are regarded as homogeneous bars, and according to Equations (1) and (2), the inertial force and torque of each bar can be expressed as follows:

(1) Inertia force and torque of branch U:

$$f_1 = -m_1 a_1, \quad T_1 = -\left[I_1^o\right]\varepsilon_1 - \left[\omega_1\right]\left[I_1^o\right]S\left(\omega_1\right) \tag{3}$$

(2) Inertia force and torque of upper Branch UPS:

$$f_{0iu} = -m_{0iu} a_{0iu}, \quad T_{0iu} = -\left[I_{0iu}^o\right]\varepsilon_{0iu} - \left[\omega_{0iu}\right]\left[I_{0iu}^o\right]S\left(\omega_{0iu}\right) \quad (i = 1, 2) \tag{4}$$

(3) Inertia force and torque of down Branch UPS:

$$f_{0id} = -m_{0id} a_{0id}, \quad T_{0id} = -\left[I_{0id}^o\right]\varepsilon_{0id} - \left[\omega_{0id}\right]\left[I_{0id}^o\right]S\left(\omega_{0id}\right) \quad (i = 1, 2) \tag{5}$$

(4) Inertia force and torque of branch R:

$$f_2 = -m_2 a_2, \quad T_2 = -\left[I_2^o\right]\varepsilon_2 - \left[\omega_2\right]\left[I_2^o\right]S\left(\omega_2\right) \tag{6}$$

3.2. **The active force and the reaction force of the upper leg mechanism.** Suppose the end point P of the robot's leg is subjected to external force and external torque, including inertial force and torque, it can be simplified into a six-dimensional force vector to the centroid. Also, the external forces of the fixed platform and other components which are mainly inertial force and torque, can be simplified into six-dimensional force vector to the centroid. The total external forces F_k of each component in the fixed coordinate system, can be written as follows:

$$f = \begin{bmatrix} f_x & f_y & f_z \end{bmatrix}^{\mathrm{T}}, \quad T = \begin{bmatrix} T_x & T_y & T_z \end{bmatrix}^{\mathrm{T}} \tag{7}$$

In the same way, the reaction force of each motion pair can be decomposed along the coordinate system and can be expressed as follows:

$$F_r = \left(f_r \;\; T_r\right)^{\mathrm{T}} = \begin{pmatrix} f_{rx} & f_{ry} & f_{rz} & T_{rx} & T_{ry} & T_{rz} \end{pmatrix}^{\mathrm{T}} \tag{8}$$

For different motion pairs, the components are subjected to different constraint forces and torques. For example, the U-pair has 2 DOF, so it is subjected to 4 constraint reaction forces and torques; the S-pair has 3 DOF, so it is subjected to 3 constrained reaction forces; the R-pair and P-pair both have only 1 DOF, so they are subjected to 5 constraint reaction forces and torques.

According to the above theoretical analysis, in order to obtain the active force and torque of each component of the leg mechanism and the constraint reaction force and torque of all the motion pairs, the entire UPS branch, the lower part of the UPS branch, the U branch and the R branch are selected as the research objects. The statics equilibrium equations of the four parts can be established respectively, and the forces and torques of each part are shown in Figure 3 and Figure 4.

Figure 3 shows the force analysis of the UPS branch and PS branch. As shown in Figure 3(a), the UPS branch is subjected to 4 unknown constraint forces and torques $f_{Al_{0i}x}$, $f_{Al_{0i}y}$, $f_{Al_{0i}z}$ and $T_{Al_{0i}z}$ at the center point of the Hooke hinge, 3 unknown constraint forces $f_{l_1l_{0i}x}$, $f_{l_1l_{0i}y}$ and $f_{l_1l_{0i}z}$ at the center point of the S-pair, the inertial force and torque f_u^i and T_u^i at the centroid of the upper part of the UPS, the inertia force and torque f_d^i and T_d^i at the

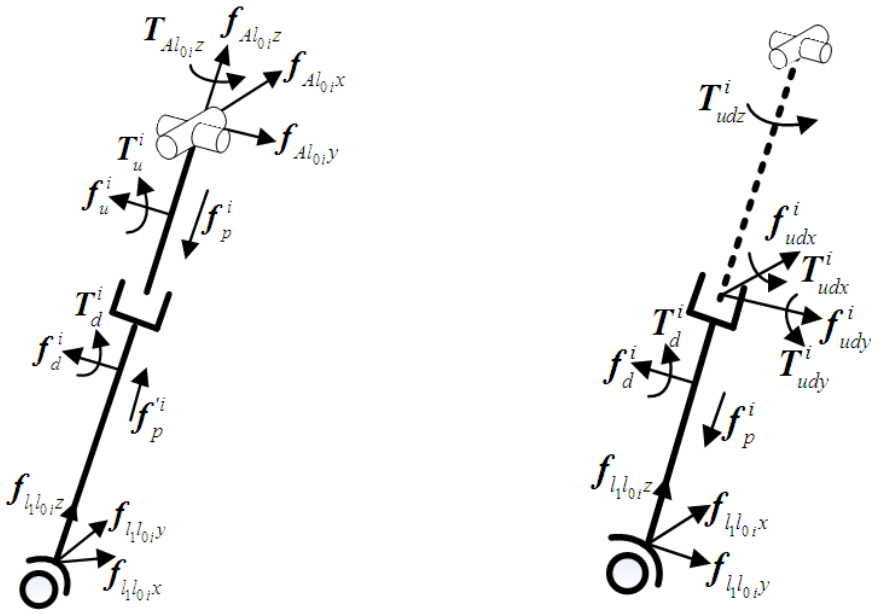

(a) Force analysis of UPS branch (b) Force analysis of PS branch

FIGURE 3. UPS branch and its lower part force analysis

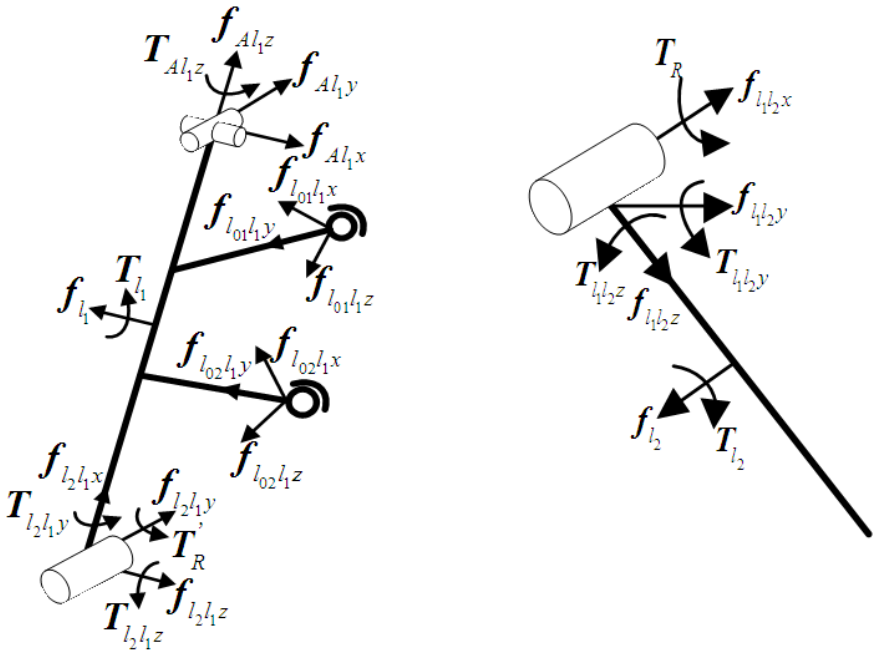

(a) Force analysis of U branch (b) Force analysis of R branch

FIGURE 4. Force analysis of U branch and R branch

centroid of the lower part of the UPS, and the propulsive force of the push rod f_p^i and $f_p^{'i}$ where f_p^i and $f_p^{'i}$ are the internal forces of equal and opposite acting at the same point.

As shown in Figure 3(b), the PS branch is the lower part of the UPS branch, and it is subjected to 5 unknown constraint forces and torques f_{udx}^i, f_{udy}^i, T_{udx}^i, T_{udy}^i and T_{udz}^i at the center point of the P-pair, the propulsive force of the push rod f_p^i, the inertia force and torque f_d^i and T_d^i at the centroid of the lower part of the UPS, and 3 unknown constraint forces $f_{l_1l_{0i}x}$, $f_{l_1l_{0i}y}$ and $f_{l_1l_{0i}z}$ at the center point of the S-pair.

The analysis above shows that the static equilibrium equations of the two branches can be transformed and arranged into matrix form as follows:

$$\begin{bmatrix} 1 & 0 & 0 & 1 & 0 & 0 & 0 \\ 0 & 1 & 0 & 0 & 1 & 0 & 0 \\ 0 & 0 & 1 & 0 & 0 & 1 & 0 \\ 0 & l_{0i} & 0 & 0 & 0 & 0 & 0 \\ -l_{0i} & 0 & 0 & 0 & 0 & 0 & 0 \\ 0 & 0 & 0 & 0 & 0 & 0 & 1 \end{bmatrix} \begin{bmatrix} f_{Al_{0i}x} \\ f_{Al_{0i}y} \\ f_{Al_{0i}z} \\ f_{l_1l_{0i}x} \\ f_{l_1l_{0i}y} \\ f_{l_1l_{0i}z} \\ T_{Al_{0i}z} \end{bmatrix} = \begin{bmatrix} f_{ux}^i + f_{dx}^i \\ f_{uy}^i + f_{dy}^i \\ f_{uz}^i + f_{dz}^i \\ \left(\frac{1}{2}l_{0iu} + l_{0id}\right) \times f_{uy}^i + \frac{1}{2}l_{0id} \times f_{dy}^i + T_{ux}^i + T_{dx}^i \\ -\left(\frac{1}{2}l_{0iu} + l_{0id}\right) \times f_{ux}^i - \frac{1}{2}l_{0id} \times f_{dx}^i + T_{uy}^i + T_{dy}^i \\ T_{uz}^i + T_{dz}^i \end{bmatrix} \tag{9}$$

$$\begin{bmatrix} 1 & 0 & 0 & 0 & 0 & 0 \\ 0 & 1 & 0 & 0 & 0 & 0 \\ 0 & 0 & 1 & 0 & 0 & 0 \\ 0 & l_{0id} & 0 & 1 & 0 & 0 \\ -l_{0id} & 0 & 0 & 0 & 1 & 0 \\ 0 & 0 & 0 & 0 & 0 & 1 \end{bmatrix} \begin{bmatrix} f_{udx}^i \\ f_{udy}^i \\ f_p^i \\ T_{udx}^i \\ T_{udy}^i \\ T_{udz}^i \end{bmatrix} = \begin{bmatrix} f_{dx}^i - f_{l_1l_{0i}x} \\ f_{dy}^i - f_{l_1l_{0i}y} \\ f_{dz}^i - f_{l_1l_{0i}z} \\ \frac{1}{2}l_{0id} \times f_{dy}^i + T_{dx}^i \\ -\frac{1}{2}l_{0id} \times f_{dx}^i + T_{dy}^i \\ T_{dz}^i \end{bmatrix} \tag{10}$$

Equations (9) and (10) include 13 unknown constraint reaction forces and drive propulsive forces, so the two UPS branches have 26 unknowns altogether, and the four components can list 24 relational equations.

Figure 4 shows the force analysis of the U branch and the R branch. As shown in Figure 4(a), the U branch is subjected to 4 unknown constraint forces and torques f_{Al_1x}, f_{Al_1y}, f_{Al_1z} and T_{Al_1z} at the center point of the Hooke hinge, 5 unknown constraint forces and torques $f_{l_2l_1x}$, $f_{l_2l_1y}$, $f_{l_2l_1z}$, $T_{l_2l_1y}$ and $T_{l_2l_1z}$ at the center point of the R-pair, 6 unknown constraint forces $f_{l_{01}l_1x}$, $f_{l_{01}l_1y}$, $f_{l_{01}l_1z}$, $f_{l_{02}l_1x}$, $f_{l_{02}l_1y}$ and $f_{l_{02}l_1z}$ at the center point of the two S-pair and the inertial force and torque f_{l_1} and T_{l_1} at the centroid of the U-branch.

As shown in Figure 4(b), the R branch is subjected to 5 unknown constraint forces and torques $f_{l_1l_2x}$, $f_{l_1l_2y}$, $f_{l_1l_2z}$, $T_{l_1l_2y}$ and $T_{l_1l_2z}$, the external force and torque f_{l_2} and T_{l_2} at the centroid of R-branch, including the inertial force and torque, and the driving torque T_R at the center point of the R-pair.

The U branch and R branch contain 21 unknown constraint reaction forces and driving torque altogether, and can list 12 relational equations. The static equilibrium equations can be transformed and arranged into matrix form as follows:

$$\begin{bmatrix} 1 & 0 & 0 & 1 & 0 & 0 & 1 & 0 & 0 & 0 \\ 0 & 1 & 0 & 0 & 1 & 0 & 0 & 1 & 0 & 0 \\ 0 & 0 & 1 & 0 & 0 & 1 & 0 & 0 & 1 & 0 \\ 0 & l_1 & 0 & 0 & l_1 - l_{11} & 0 & 0 & l_1 - l_{12} & l_c & 0 \\ -l_1 & 0 & 0 & l_{11} - l_1 & 0 & -l_b & l_{12} - l_1 & 0 & 0 & 0 \\ 0 & 0 & 0 & 0 & l_b & 0 & -l_c & 0 & 0 & 1 \end{bmatrix} \begin{bmatrix} f_{Al_1x} \\ f_{Al_1y} \\ f_{Al_1z} \\ f_{l_{01}l_1x} \\ f_{l_{01}l_1y} \\ f_{l_{01}l_1z} \\ f_{l_{02}l_1x} \\ f_{l_{02}l_1y} \\ f_{l_{02}l_1z} \\ T_{Al_1z} \end{bmatrix}$$

$$= \begin{bmatrix} f_{l_1x} - f_{l_2l_1x} \\ f_{l_1y} - f_{l_2l_1y} \\ f_{l_1z} - f_{l_2l_1z} \\ \frac{1}{2}l_1 \times f_{l_1y} + T_{l_1x} - T'_R \\ -\frac{1}{2}l_1 \times f_{l_1x} + T_{l_1y} - T_{l_2l_1y} \\ T_{l_1z} - T_{l_2l_1z} \end{bmatrix} \tag{11}$$

$$\begin{bmatrix} 1 & 0 & 0 & 0 & 0 & 0 \\ 0 & 1 & 0 & 0 & 0 & 0 \\ 0 & 0 & 1 & 0 & 0 & 0 \\ 0 & \frac{1}{2}l_2 & 0 & 1 & 0 & 0 \\ -\frac{1}{2}l_2 & 0 & 0 & 0 & 1 & 0 \\ 0 & 0 & 0 & 0 & 0 & 1 \end{bmatrix} \begin{bmatrix} f_{l_1l_2x} \\ f_{l_1l_2y} \\ f_{l_1l_2z} \\ T_R \\ T_{l_1l_2y} \\ T_{l_1l_2z} \end{bmatrix} = \begin{bmatrix} f_{l_2x} \\ f_{l_2y} \\ f_{l_2z} \\ T_{l_2x} \\ T_{l_2y} \\ T_{l_2z} \end{bmatrix} \tag{12}$$

where $f_{l_2l_1}$, $T_{l_2l_1}$, T_R and $f_{l_1l_2}$, $T_{l_1l_2}$, T'_R are the force/torque and reaction force/torque in different coordinate systems. $f_{l_{01}l_1}$, $f_{l_{02}l_1}$ and $f_{l_1l_{01}}$, $f_{l_1l_{02}}$ are also the force and reaction force in different coordinate systems. The rotation transformation matrix of the two UPS branches relative to the U branch is known as:

$${}^{l_1}_{l_{01}}R = \begin{bmatrix} c\beta_{01} & 0 & s\beta_{01} \\ 0 & 1 & 0 \\ -s\beta_{01} & 0 & c\beta_{01} \end{bmatrix}, \qquad {}^{l_1}_{l_{02}}R = \begin{bmatrix} 1 & 0 & 0 \\ 0 & c\alpha_{02} & -s\alpha_{02} \\ 0 & s\alpha_{02} & c\alpha_{02} \end{bmatrix} \tag{13}$$

Then the relationship can be obtained

$$\begin{bmatrix} f_{l_2l_1} \\ T_{l_2l_1} \end{bmatrix} = \begin{bmatrix} {}^{l_1}_{l_2}R & 0 \\ S\left({}^{l_1}P_{l_2}\right){}^{l_1}_{l_2}R & {}^{l_1}_{l_2}R \end{bmatrix} \begin{bmatrix} -f_{l_1l_2} \\ -T_{l_1l_2} \end{bmatrix} \qquad \begin{bmatrix} f_{l_{01}l_1} \\ f_{l_{02}l_1} \end{bmatrix} = \begin{bmatrix} {}^{l_1}_{l_{01}}R & 0 \\ 0 & {}^{l_1}_{l_{02}}R \end{bmatrix} \begin{bmatrix} -f_{l_1l_{01}} \\ -f_{l_1l_{02}} \end{bmatrix} \tag{14}$$

From Equations (9) to (14), there are 47 unknown quantities, 36 independent equations and 11 relation expressions between force/torque and reaction force/torque in different coordinate systems. Therefore, when the external force F and torque T are known, and putting them into Equation (12), then the constraint reaction force/torque and the driving torque in all directions of the R-pair can be obtained. Then the results are substituted into Equations (11), (10) and (9), and the constraint reaction force/torque and driving forces of other joints are obtained by solving the linear equations.

From the static equilibrium equations of each rod above, it can be seen that compared with the external force, the inertia force and the driving force of each rod, the constraint forces/torques of the joints are enough to influence the overall performance of the mechanism. Therefore, when analyzing the stiffness of the mechanism, the influence of the constraint forces/torques of each joint should be considered.

4. **Example.** Suppose the end point P of the robot's leg is subjected to external force and external torque, for example, $F = [\ 30\ \ 20\ \ 15\ ]$ and $T = [\ 1.2\ \ 1.4\ \ 2\ ]$. Then according to Equations (9) to (14), the constraint forces and torques of each joint can be obtained, as shown in Table 1.

TABLE 1. Constraint forces and torques of each joint

	f_x/N	f_y/N	f_z/N	T_x/N · m	T_y/N · m	T_z/N · m
U-pair 1	−61.80	−60.63	−363.55	–	–	11.59
U-pair 2	0	0	472.69	–	–	0
U-pair 3	0	0	−110.70	–	–	0
S-pair 1	0	0	−472.69	–	–	–
S-pair 2	0	0	110.70	–	–	–
R-pair 1	30	20	15	–	5.75	2

Substituting the numerical values into Equation (12), the driving torque T_R can be obtained, which is 1.7 N · m. The constraint reaction torques in Y and Z direction of the R-pair are 5.75 N · m and 2 N · m respectively. From the above data, it can be seen that the constraint reaction torque in Y and Z direction of the R-pair are bigger than the driving torque in X direction. Therefore, when considering the stiffness and the material of the mechanism, not only consider whether it can bear the maximum driving torque, but also be able to bear the constrained reaction torque.

5. **Conclusions.** In this paper, the main structure of the leg-wheeled rescue robot is developed, which is composed of the front and rear frame and four same structure leg mechanism. The most special part of this robot is that each leg has three degrees of freedom (3-DOF) with serial-parallel mechanism (2-UPS+U) & R, which has the advantages of high speed and obstacle-surmounting. Its flexibility and the carrying ability have been improved greatly. The inertia force/torque of each member of the leg mechanism is analyzed, and the mechanical balance equation of each member is solved, and the relation expression of each joint's constraint/torque, driving force and the end of the machine is analyzed.

In the future, the prototype of the rescue robot will be finished. The static analysis will provide the theoretical foundation for further research on optimum design and selection of materials.

Acknowledgment. This work is partially supported by EU H2020 Project – SMOOTH (Project No. 734875), and the collaborative innovation project of college of mechanical engineering, Yanshan University, Hebei Province (Project No. JX2014-01). The authors also gratefully acknowledge the helpful comments and suggestions of the reviewers, which have improved the presentation.

REFERENCES

[1] I. Tanev, Learning mutation strategies for evolution and adaptation of a simulated Snakebot, in *Advances in Applied Self-Organizing Systems*, 2nd Edition, Springer, London, 2013.

[2] I. Tanev, Genetic programming incorporating biased mutation for evolution and adaptation of Snakebot, *Genetic Programming and Evolvable Machines*, vol.8, no.1, pp.39-59, 2007.

[3] N. Mukosaka, I. Tanev and K. Shimohara, Performance of incremental genetic programming on adaptability of snake-like robot, *Procedia Computer Science*, vol.24, pp.152-157, 2013.

[4] E. Rohmer, K. Ohno and T. Yoshida, Integration of a sub-crawlers' autonomous control in quince highly mobile rescue robot, *IEEE/SICE International Symposium on System Integration*, pp.78-83, 2010.

[5] T. Yoshida, K. Nagatani, S. Tadokoro et al., Improvements to the rescue robot quince toward future indoor surveillance missions in the Fukushima Daiichi nuclear power plant, *Field and Service Robotics*, vol.92, pp.19-32, 2014.

[6] G. Endo and S. Hirose, Study on Roller-Walker (multi-mode steering control and self-contained locomotion), *Proc. of the ICRA Conference on Robotics and Automation*, no.3, pp.2808-2814, 2000.

[7] E. Gen and S. Hirose, Study on Roller-Walker improvement of locomotive efficiency of quadruped robots by passive wheels, *Advanced Robotics*, vol.26, nos.8-9, pp.969-988, 2012.

[8] S. R. Gourley, PackBot, *Army*, vol.55, no.2, pp.78-79, 2005.

[9] R. R. Murphy, S. Tadokoro and A. Kleiner, Disaster robotics, *Springer Handbook of Robotics*, 2nd Edition, pp.1577-1604, 2016.

[10] H. J. Eisen, L. C. Wen, G. Hickey et al., Sojourner Mars rover thermal performance, *The 28th International Conference on Environmental Systems*, p.13, 1998.

[11] B. H. Wilcox, T. Litwin, J. Biesiadecki et al., Athlete: A cargo handling and manipulation robot for the moon, *Journal of Field Robotics*, vol.24, no.5, pp.421-434, 2007.

[12] C. Grand, F. B. Amar, F. Plumet et al., Stability and traction optimization of a reconfigurable wheel-legged robot, *International Journal of Robotics Research*, vol.23, nos.10-11, pp.1041-1058, 2004.

[13] Y. Luo, Q. Li and Z. Liu, Design and optimization of wheel-legged robot: Rolling-wolf, *Chinese Journal of Mechanical Engineering (English Edition)*, vol.27, no.6, pp.1133-1142, 2014.

[14] E. Rohmer, M. Collins, G. Reina and K. Yoshida, A novel teleoperated hybrid wheel-limbed hexapod for the exploration of lunar challenging terrains, *International Symposium on Space Technology and Science*, pp.3902-3907, 2008.

[15] M. Qu, H. Wang and Y. Rong, Statics performance evaluating and optimal design of a parallel mechanical leg of the wheel-leg hybrid quadruped robot, *ICIC Express Letters, Part B: Applications*, vol.8, no.7, pp.1041-1049, 2017.

[16] G. Shanmugasundar, R. Sivaramakrishnan and S. Venugopal, Modeling, design and static analysis of seven degree of freedom articulated inspection robot, *Advanced Materials Research*, vol.657, pp.1053-1056, 2013.